

**MJEN**

Synthesize of montmorillonite supported hydroxyapatite and determination of adsorption capacity by tetracycline removal

Pelin Demircivi

Kimya Mühendisliği Bölümü, Mühendislik Fakültesi, Yalova Üniversitesi, Yalova, Türkiye, pelin.demircivi@yalova.edu.tr,
ORCID: 0000-0002-1068-9310

ABSTRACT

In this study, removal of organic pollutants in wastewater using HA/MMT composite material was studied. Tetracycline (TC) antibiotic was used as an organic pollutant. HA/MMT composites were synthesized in a ball mill at different ratios (1:1, 1:2 and 2:1). The synthesis time was fixed at 5 hours. As a result of the experiments, it was concluded that 1:2 ratio of HA/MMT composite has the highest adsorption capacity (147 mg g^{-1}) among the others. The isotherm experiments showed that the Langmuir isotherm model was compatible with the experimental data, and the maximum adsorption capacity was obtained as 150 mg g^{-1} , which indicated that TC was adsorbed to create a monolayer coverage on HA/MMT adsorption sites. In the light of kinetic data, pseudo-second-order kinetic model was the best suitable model for TC adsorption; moreover the calculated adsorption capacity ($q_e = 227.27 \text{ mg g}^{-1}$) was found suitable with experimental ($q_e = 223.47 \text{ mg g}^{-1}$). In addition, it has been observed that intra-particle diffusion takes place as a rate-determining step. It has been concluded that TC adsorption of HA/MMT composite was an endothermic ($\Delta H^\circ = +39.85 \text{ kJ mol}^{-1}$) and spontaneous process thermodynamically. It has been concluded that the synthesized HA/MMT composite has high adsorption capacity and can be used for the removal of organic pollutants such as TC from wastewater.

ARTICLE INFO

Research article

Received: 14.09.2022

Accepted: 12.12.2022

Keywords:

Hydroxyapatite,
montmorillonite,
clay composites,
removal of antibiotics

1. Introduction

Tetracycline (TC) is an antibiotic with broad-spectrum antimicrobial activity. Therefore, it is a type of antibiotic frequently used in the treatment of both human and animals [1]. TC, which is not fully metabolized in human and animal bodies, can easily penetrate into soil and water system. Antimicrobial resistance occurs with the increasing amount of TC in the environment and this situation is reflected in the food chain and causes environmental effects [2]. Therefore, TC removal from wastewater is of great importance.

Conventional methods for wastewater treatment are not sufficient for the removal of antibiotics. Therefore, advanced treatment methods are used in the treatment of wastewater. Adsorption is a widely used treatment method among advanced treatment methods with its low cost, high efficiency and easy applicability, which has also some disadvantages such as waste production and low selectivity [3]. Materials such as activated carbon, polymeric materials, clay, and biochar have been used as adsorbent in the removal of TC from wastewater [4-6].

Hydroxyapatite (HA) is a calcium phosphate material with the chemical formula $\text{Ca}_{10}(\text{PO}_4)_6(\text{OH})_2$. HA is a chemically

stable, low-solubility and non-toxic material with having high porosity. In addition, it is used in adsorption studies due to its high adsorption capacity [7]. Active adsorption sites on HA are cationic and anionic Ca^{2+} and PO_4^{3-} groups. The disadvantage of using HA in treatment processes is its low reusability due to its low mechanical strength. Various materials such as clay, chitosan, and carbon nanotubes are added to its structure to increase its mechanical strength [8-10]. Clay minerals are preferred due to their low cost, non-toxicity, and high adsorption capacity [11, 12]. Ofudje et al. (2021) studied removal of nickel using nano-rod hydroxyapatite, which was synthesized via thermal decomposition method. Adsorption studies showed that maximum removal of Ni^{2+} was found 183 mg g^{-1} while thermal decomposition temperature was 900°C [13]. Peng et al. (2023) investigated adsorption of Cu^{2+} by hydroxyapatite synthesized from marble sludge. Eco-friendly hydroxyapatite was synthesized by hydrothermal method and maximum adsorption capacity was achieved 256 mg g^{-1} [14]. Wei et al. (2021) examined adsorption of tannic acid by hydroxyapatite with a maximum adsorption capacity of 95 mg g^{-1} [15]. According to a brief literature research, hydroxyapatite and its clay modification form has not been used for removal of antibiotics from aqueous solution.

In this study, HA/MMT adsorbent was synthesized by adding montmorillonite (MMT) clay into the HA structure and used for TC removal. The effects of adsorbent amount, pH, contact time and temperature on TC removal were studied. In the light of the obtained data, adsorption capacity, kinetic and isotherm models were obtained and the adsorption mechanism was clarified.

2. Materials and methods

Montmorillonite (MMT) was received from Kalemaden Ceramic Factory at Canakkale (The chemical composition of MMT: SiO₂: 71%, Al₂O₃: 16%, TiO₂: 0.2%, Fe₂O₃: 1.5%, CaO: 2%, MgO: 2%, Na₂O: 1%, K₂O: 0.5%). The HA used in the experiments was obtained from Xi'an Realin Biotechnology. The HA used has a purity of 99% and the impurities in its structure are indicated in Table 1. All the reagents were in analytical grade.

Table 1. Impurities in the HA structure

Sulphate (%)	Chloride (%)	Heavy metals (mg L ⁻¹)
<0,048	<0,05	<10

Composites containing HA and MMT in different ratios (1:1, 1:2 and 2:1) were prepared. HA/MMT composites were obtained by grinding in a ball mill for 5 hours. In order to determine the amount of adsorbent and HA/MMT ratio to be used in the experiments, 1-30 mg of HA/MMT composites were weighed and shaken in an orbital shaker for 24 hours with 25 mL of 20 mg L⁻¹ TC solution. pH experiments were carried out using the determined HA/MMT ratio and adsorbent amount. In order to determine the most suitable pH value for TC adsorption, the pH value of the TC solution was adjusted between 2-12 using 0.1 M HCl and 0.1 M NaOH solutions. The determined amount of HA/MMT composite and 25 mL of 20 mg L⁻¹ TC solution was shaken in an orbital shaker for 24 hours. In contact time trials, samples were collected and analyzed between 0-300 min. In order to determine the thermodynamic parameters, adsorption experiments were carried out at 25, 35 and 45 °C. Samples taken at the end of all experiments were first filtered through a filter with a pore diameter of 0.45 µm and spectrophotometric measurements were made by UV-visible spectrophotometer (Shimadzu UV-Vis-1800) at 360 nm, the highest wavelength of the TC solution. Arithmetically averaging of triplicate experiments were utilized to fit

adsorption curves. Adsorption capacity was calculated using Eq.1 from obtained data.

$$q_e = \frac{C_o - C_e}{m} xV \quad (1)$$

Here, q_e is the adsorption capacity at equilibrium (mg g⁻¹), C_o and C_e are the TC concentration at initial and equilibrium (mg L⁻¹), m is the amount of adsorbent (g), and V is the solution volume.

3. Results and discussion

3.1. Effect of HA/MMT ratio and adsorbent amount on TC adsorption

In order to examine the effect of HA and MMT on TC adsorption, composites containing HA and MMT in 1:1, 1:2 and 2:1 ratios were synthesized. Experiments were carried out using 25 mL of 20 mg L⁻¹ TC solution and the amount of adsorbent was used between 1-30 mg. In Figure 1, the adsorption capacity and adsorption efficiency values against the amount of adsorbent were shown. According to Figure 1, the adsorption efficiency increased with the increase in the amount of adsorbent. Adsorption efficiency of 27%, 32% and 23% for 1 mg adsorbent amount was obtained for composites containing HA and MMT at 1:1, 1:2 and 2:1 ratios, while these values were 80%, 91% and 71%, respectively, for 30 mg adsorbent amount. Since the increase in the amount of adsorbent causes an increase in the adsorption surface, it also causes an increase in the active adsorption sites where TC adsorption will take place, and TC adsorption increases. In addition, the appropriate amount of adsorbent to be used in the experiments was determined as 20 mg, and the adsorption capacities were obtained as 24, 26 and 21 mg g⁻¹, respectively, against the amount of adsorbent. The reason for choosing the appropriate amount of adsorbent as 20 mg is that there is no change in adsorption efficiency despite increasing the amount of adsorbent and the adsorbent cannot adsorb more TC. Therefore, 20 mg adsorbent amount was used for all three adsorbents in the experiments.

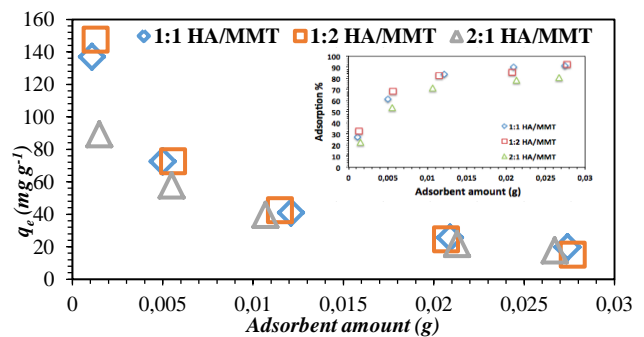


Figure 1. Adsorption capacity and adsorption efficiency against the amount of adsorbent belonging to different HA/MMT ratios

When HA/MMT ratios were compared, the highest yield was obtained at 1:2 ratio (91%), while lower adsorption efficiency was obtained at 1:1 and 2:1 ratios (80% and 71%), respectively. Since TC has both positive and negative sites due to its structure, it was concluded that adsorption occurred with electrostatic interaction on the MMT surface and hydroxyl (-OH), calcium (Ca^{2+}) and phosphate (PO_4^{3-}) groups in the HA structure were also effective in adsorption. 1:2 HA/MMT adsorbent, where the highest adsorption efficiency was obtained, was used in parameter trials.

3.2 Effect of pH on TC adsorption

One of the most important parameters affecting the adsorption is the pH value of the solution, as it causes changes in both the adsorbate types and the surface properties of the adsorbent. The initial solution pH values of 25 mL of 20 mg L^{-1} TC solution were changed in the range of 2-12 and adsorption experiments were carried out using $20 \text{ mg HA/MMT}(1:2)$ adsorbent. As a result of the experiments, it was observed that the highest removal was realized around pH 6 and the adsorption efficiency was obtained as 95% at this pH value (Figure 2). While the adsorption efficiency in strongly acidic solution (pH=2) was 67%, respectively, it was observed that it decreased to 49% in strongly basic area (pH=12). The adsorption capacity was obtained as 19 mg g^{-1} and 20 mg g^{-1} at pH 2 and 12, respectively. At pH 6, where the highest removal was achieved, the adsorption capacity was 26 mg g^{-1} .

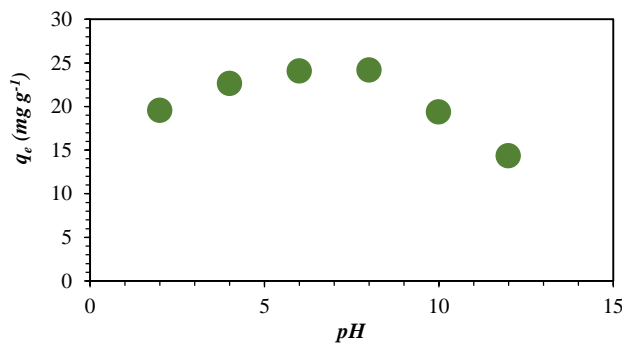


Figure 2. Effect of solution pH value on TC adsorption

In TC aqueous solution, it can exist in different structural forms depending on the pH of the solution. TC has three different dissociation constants; these are designated as $pK_{a1}=3.3$ (dimethylamino group), $pK_{a2}=7.3-7.7$ (phenolic diketone group), and $pK_{a3}=9.1-9.7$ (tri-carbonylamide group) [4]. While the cationic TC form (TCH_3^+) is dominant in the aqueous solution at pH 3.3, it comes to the TCH_2^\pm form where the positive and negative charge density is equal between pH 3.3-7.7. In the basic environment where the pH value is higher than 7.7, TCH^- and TC_2^- forms are present in the aqueous solution as negatively charged ions [16, 17]. In the light of this information, at pH 6, where the highest removal is achieved, C contains both positive and negative

charges and it is known that the total charge density is zero. The isoelectric point for HA/MMT adsorbent is around 6.6. The HA/MMT adsorbent is positively charged when the solution pH is lower than the isoelectric point, and negatively charged when it is higher. The adsorption value was found to be low, as there would be an electrostatic repulsion force between the positively charged adsorbent and the positively charged TC molecule (TCH_3^+) in an acidic environment. Adsorption increased when the pH value was around the isoelectric point. In this region, TC is in the TCH_2^\pm structure in aqueous solution and adsorption takes place by electrostatic attraction between its charged groups and HA/MMT adsorbent. In addition, TC, which has high hydrophobicity, can be adsorbed on the adsorbent surface with the hydrophobic interactions it will form. In basic media, adsorption decreases partially due to the repulsive force between the negatively charged adsorbent surface and TCH^- and TC_2^- molecules [18].

3.3 Adsorption isotherm

Adsorption isotherms were created to determine the TC adsorption capacity of HA/MMT adsorbent. As indicated in Figure 3, while the adsorption capacity of the 1:2 ratio HA/MMT composite was the highest (147 mg g^{-1}), the lowest adsorption capacity was obtained at the 2:1 HA/MMT ratio (89 mg g^{-1}). Experimentally obtained data were analyzed using Langmuir, Freundlich and Temkin isotherm models and the mechanism of TC adsorption at the solid/liquid interface was revealed.

Langmuir isotherm model assumes that the adsorption occurs on homogenous surface sites on the adsorbent and monolayer coverage occurs on the same adsorption energy sites. The linear form of the Langmuir isotherm equation is given in Eq. (2);

$$\frac{C_e}{q_e} = \frac{1}{Qb} + \frac{C_e}{Q} \quad (2)$$

where q_e is the amount of TC adsorbed at equilibrium (mg g^{-1}), C_e is the equilibrium TC concentration in the solution (mg L^{-1}), Q is the monolayer capacity of the adsorbent (mg g^{-1}) and b is the Langmuir adsorption constant (L mg^{-1}).

Freundlich isotherm model takes place on heterogeneous surface sites with non-uniform distribution of sorption heat. Multilayer coverage occurs on heterogenous surface sites. The linear form of the Freundlich isotherm equation is given in Eq. (3);

$$\log q_e = \log K_f + \frac{1}{n} \log C_e \quad (3)$$

where q_e is the amount of TC adsorbed at equilibrium (mg g^{-1}), C_e is the equilibrium TC concentration in the solution (mg L^{-1}), K_f is Freundlich constant related to the adsorption

capacity ($L g^{-1}$) and n is the Freundlich constant related to adsorption intensity.

Temkin isotherm model describes linear decline of adsorption heat instead of logarithmic decline. Linearized form of Temkin isotherm expressed as (4);

$$q_e = \frac{RT}{b} \ln K_t + \frac{RT}{b} \ln C_e \quad (4)$$

where q_e is the amount of boron adsorbed at equilibrium ($mg g^{-1}$), C_e is the equilibrium boron concentration in the solution ($mg L^{-1}$), K_t is the equilibrium binding constant ($L g^{-1}$), b is the Temkin constant, R is the ideal gas constant and T is the temperature.

According to the obtained data, when the correlation coefficients (R^2) of the studied models were compared, it was found that the Langmuir isotherm model (0.98) was compatible with TC adsorption (Table 2). In this case, it was concluded that the TC molecule was adsorbed on the HA/MMT surface as a single layer. It was concluded that the maximum adsorption capacity ($150 mg g^{-1}$) obtained from Table 2. Isotherm models of different HA/MMT ratios

Adsorbent	Langmuir isotherm			Freundlich isotherm		Temkin isotherm			
	Q_m ($mg g^{-1}$)	b	R^2	K_F ($mg g^{-1}$)	n	R^2	K_t ($L g^{-1}$)	b	R^2
1 HA : 1 MMT	138,89	0,0153	0,97	11,292	1,13	0,98	0,0005	0,045	0,91
1 HA : 2 MMT	150,00	0,1782	0,85	3,285	0,74	0,88	0,0012	0,030	0,86
2 HA : 1 MMT	100,11	0,0019	0,93	3,548	0,87	0,95	0,0012	0,048	0,99

Electrostatic and hydrophobic interactions dominate the adsorption of the TC molecule on the HA/MMT surface, while hydrogen bonds are also effective in TC adsorption. The oxygen atoms in the carboxyl and hydroxyl groups in the TC structure provide the formation of dipole-dipole H bonds on the HA/MMT surface. In addition, Si-OH, Al-OH groups and Ca-OH, P-OH groups in the HA/MMT structure play an important role in TC adsorption [23, 24].

3.4 Adsorption kinetics

In order to examine the adsorption kinetics, samples were taken at different time intervals (0-300 min) and a graph of adsorption capacity at equilibrium was obtained (Figure 4). It was observed that the adsorption on the HA/MMT (1:2) surface of the TC molecule reached equilibrium in 180 minutes. In the first 120 minutes, the TC molecule was adsorbed on the HA/MMT surface rapidly, while the amount of adsorption did not change at the end of 180 minutes. In the first 120 minutes, when rapid adsorption is observed, empty adsorption sites are quickly filled with TC molecules, and as the time progresses, the adsorption capacity decreases as all of the adsorption sites are filled.

the Langmuir isotherm model was in agreement with the experimentally obtained data ($147 mg g^{-1}$). Moreover, tetracycline adsorption capacity of 1:2 HA/MMT was much higher than $32 mg g^{-1}$ on illite [19], $140 mg g^{-1}$ on rectorite [20], $4 mg g^{-1}$ on kaolinite [21] and $11 mg g^{-1}$ on MMT-biochar [22].

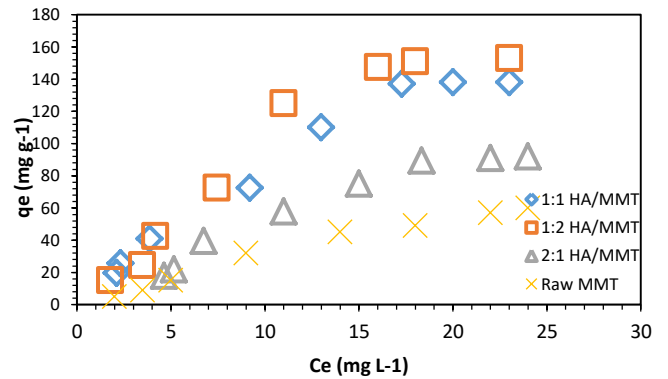


Figure 3. Isotherm plot of different HA/MMT ratios

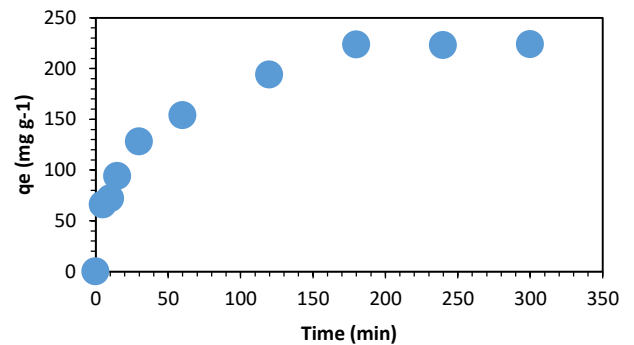


Figure 4. Variation of HA/MMT adsorption capacity versus time Pseudo-first-order, pseudo-second-order kinetic models and intra-particle diffusion model were applied to analyze the kinetic data. The pseudo-first order rate equation of Lagergren is given in Eq. (5);

$$\log(q_e - q_t) = \log q_e - \frac{k_1}{2.303} t \quad (5)$$

where q_e and q_t are the amounts of adsorbed TC at equilibrium and at time t (mg g^{-1}) and k_1 is the pseudo-first-order rate constant (min^{-1}).

The pseudo-second-order rate equation is given in Eq. (6);

$$\frac{t}{q_t} = \frac{1}{k_2 q_e^2} + \frac{1}{q_e} t \tag{6}$$

where q_e and q_t are the amounts of adsorbed TC at equilibrium and time t (mg g^{-1}) and k_2 is the pseudo-second-order rate constant ($\text{g mg}^{-1} \text{min}^{-1}$).

The intra-particle diffusion model is given in Eq. (7);

$$q_t = k_{int} t^{1/2} + c \tag{7}$$

where q_t is the amount of adsorbed TC at time t (mg g^{-1}), k_{int} is the intra-particle-diffusion rate constant ($\text{mg g}^{-1} \text{min}^{-1/2}$), t is the time (min) and c is the intercept (mg g^{-1}).

The parameters of the kinetic models are given in Table 3. When the correlation coefficients (R^2) are compared, it is seen that the correlation coefficient (0.99) of the pseudo-second-order kinetic model is considerably higher than (0.91) of the pseudo-first-order kinetic model. In addition, it was concluded that the adsorption capacity calculated using the kinetic model ($q_e = 227.27 \text{ mg g}^{-1}$) was compatible with the experimentally obtained adsorption capacity ($q_e = 223.47 \text{ mg g}^{-1}$). With the intra-particle diffusion model, the mass transfer mechanism of the TC molecule from the liquid phase to the HA/MMT surface has been elucidated. According to the intra-particle diffusion model, TC adsorption consists of two steps. In the first step, diffusion of the TC molecule from the liquid phase to the HA/MMT outer surface (border layer diffusion) takes place. The second step involves diffusion and adsorption of the TC molecule into the pores on the HA/MMT surface. One of these two steps can control TC adsorption kinetically. When the k_{int1} and k_{int2} rate constants of intra-particle diffusion are compared, it is seen that the k_{int2} rate constant is much lower than the k_{int1} rate constant. Accordingly, it was concluded that intra-particle diffusion is the rate-determining step in TC adsorption [25].

Table 3. Isotherm models of TC adsorption of HA/MMT adsorbent

Pseudo first order kinetic model		
k_1 ($L dk^{-1}$)	q_e ($mg g^{-1}$)	R^2
$2,55 \cdot 10^{-2}$	25,73	0,92
Pseudo second order kinetic model		
k_2 ($g mg^{-1} dk^{-1}$)	q_e ($mg g^{-1}$)	R^2
$2,93 \cdot 10^{-3}$	227,27	0,99
Intraparticle diffusion model		
k_{int1} ($g mg^{-1} dk^{-1}$)	c	R^2
2,43	200,58	0,99
k_{int2} ($g mg^{-1} dk^{-1}$)		
0,36		

3.5 Adsorption thermodynamics

The adsorption of the TC molecule on the HA/MMT surface was investigated at different temperatures (25, 35 and 45 °C) and thermodynamic parameters were calculated from the data obtained (Table 4). Change in standard enthalpy (ΔH°) was calculated according to Van't Hoff equation;

$$\ln \left(\frac{C_{e2}}{C_{e1}} \right) = \frac{\Delta H^\circ}{R} \left(\frac{1}{T_2} - \frac{1}{T_1} \right) \tag{8}$$

Change in standard Gibbs free energy (ΔG°) was given as;

$$\Delta G^\circ = -RT \ln K \tag{9}$$

$$K = \frac{C_{ads}}{C_e} \tag{10}$$

Change in standard entropy (ΔS°) was calculated;

$$\Delta G^\circ = \Delta H^\circ - T \Delta S^\circ \tag{11}$$

Positive ΔH° value indicates that TC adsorption occurs endothermically. The fact that the ΔH° value is lower than 40 kJ mol^{-1} indicates that physical adsorption has taken place [26]. A positive ΔS° value indicates an increase in disorder at the solid/liquid interface. The negative Gibbs free energy (ΔG°) at all temperatures indicates that TC adsorption occurs spontaneously. The ΔG° value decreases as the temperature increases. This shows that the TC molecule meets the energy required to increase its diffusion and adsorb onto the HA/MMT surface [27].

Table 4. Thermodynamic parameters of HA/MMT adsorbent for TC adsorption

T	ΔH	ΔG	ΔS
---	------------	------------	------------

(K)	(kJ mol ⁻¹)	(kJ mol ⁻¹)	(J mol ⁻¹ K ⁻¹)
298		-5.49	
308	39.85	-6.61	0.165
318		-8.26	

3.6 Reusability of the adsorbent

Adsorbent stability tests were performed for 180 min using HA/MMT. At the end of each cycle, the adsorbent was separated, washed with distilled water and adsorption test was repeated at the same conditions. After third cycle, tetracycline degradation was decreased to 75%, while it was 96% for the first cycle (Fig. 5). Tetracycline adsorption after third cycle remained constant at around 64% and a decreased was observed at third cycle that could be cause of occupation of active adsorption sites by TC.

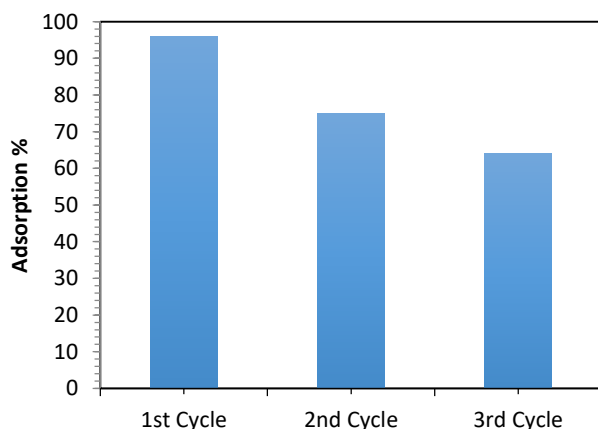


Figure 5. Reusability of 1:2 HA/MMT adsorbent

4. Conclusion

As a result of the study, it has been shown that HA/MMT adsorbent can be synthesized and used effectively in the adsorption of TC antibiotic from aqueous solutions. 1:1, 1:2 and 2:1 HA/MMT composites were synthesized and isotherm experiments were showed that 1:2 HA/MMT composite exhibited the highest adsorption capacity (147 mg g⁻¹). Moreover, the results of isotherm models were proved that 1:2 HA/MMT composition has the adsorption capacity of 150 mg g⁻¹ indicated more adsorption sites than among the other composites. As a result of kinetic models it was found that the pseudo-second order kinetic model was in agreement with the experimental data of TC adsorption ($R^2=0.99$). Thermodynamic analysis was showed that TC adsorption was a spontaneous endothermic process. It was concluded that the adsorption of the TC molecule on the HA/MMT surface occurs through electrostatic interactions, hydrophobic interactions and H-bonds. As a result of the study, it could be stated that HA-supported adsorbents can be

used effectively in the removal of antibiotics such as TC from wastewater.

References

- [1]. Chopra I., Roberts M., "Tetracycline antibiotics: Mode of action, applications, molecular biology, and epidemiology of bacterial resistance", *Microbiology and Molecular Biology Reviews*, 65, (2001), 232–260.
- [2]. Chang P.H., Jiang W.T., Li Z., Jean J.S., Kuo C.Y., "Antibiotic tetracycline in the environments-a review", *Journal of Pharmaceutical Analysis*, 4, (2015), 86-111.
- [3]. Aarab N., Hsini A., Laabd M., Essekre A., Laktif T., Ait Haki M., Lakhmiri R., Albourine A., "Theoretical study of the adsorption of sodium salicylate and metronidazole on the PANi", *Materials Today: Proceedings*, 22, (2020), 100–103.
- [4]. Anton-Herrero R., Garcia-Delgado C., Alonso-Izquierdo M., Garcia-Rodriguez G., Cuevas J., Eymar E., "Comparative adsorption of tetracyclines on biochars and stevensite: Looking for the most effective adsorbent", *Applied Clay Science*, 160, (2018), 162-172.
- [5]. Yeşilova E., Osman B., Kara A., Özer E.T., "Molecularly imprinted particle embedded composite cryogel for selective tetracycline adsorption", *Separation and Purification Technology*, 200, (2018), 155-163.
- [6]. Acosta R., Fierro V., Martínez de Yuso A., Narbalatz D., Celzard A., "Tetracycline adsorption onto activated carbons produced by KOH activation of tyre pyrolysis char," *Chemosphere*, 149, (2016), 168–176.
- [7]. Ragab A., Ahmed I., Bader D., "The removal of brilliant green dye from aqueous solution using nano hydroxyapatite/chitosan composite as a sorbent," *Molecules*, 24, (2019), 847.
- [8]. Le V.T., Doan V.D., Nguyen D.D., Nguyen H.T., Ngo Q.P., Tran T.K.N., Le H.S., "A novel cross-linked magnetic hydroxyapatite/chitosan composite: Preparation, Characterization, and Application for Ni(II) Ion Removal from Aqueous Solution", *Water, Air and Soil Pollution*, 229, (2018), 101.
- [9]. Cziko M., Bogya E.S., Paizs C., Katona G., Konya Z., Kukovecz Á., Barabás R., "Albumin adsorption study onto hydroxyapatite-multiwall carbon nanotube based

- composites”, *Materials Chemistry and Physics*, 180, (2016), 314–325.
- [10]. Hokkanen S., Doshi B., Srivastava V., Puro L., Koivula R., “Arsenic (III) removal from water by hydroxyapatite-bentonite clay-nanocrystalline cellulose”, *Environmental Progress and Sustainable Energy*, 38, (2019), 13147. ^[1]_[SEP]
- [11]. Zabihi O., Ahmadi M., Nikafshar S., Chandrakumar Preyeswary K., Naebe M., “A technical review on epoxy-clay nanocomposites: Structure, properties, and their applications in fiber reinforced composites”, *Composites Part B: Engineering*, 135, (2018), 1–24.
- [12]. El Ouardi M., Laabd M., Abou Oualid H., Brahmi Y., Abaamrane A., Elouahli A., Ait Addi A., Laknifli A., “Efficient removal of p-nitrophenol from water using montmorillonite clay: insights into the adsorption mechanism, process optimization, and regeneration”, *Environmental Science and Pollution Research*, 26, (2019), 19615–19631.
- [13]. Ofudje E.A., Adedapo A.E., Oladeji O.B., Sodiya E.F., Ibadin F.H., Zhang D., “Nano-rod hydroxyapatite for the uptake of nickel ions: Effect of sintering behaviors on adsorption parameters”, *Journal of Environmental Chemical Engineering*, 9, (2021), 105931.
- [14]. Peng S.Y., Lin Y.W., Lee W.H., Lin Y.Y., Hung M.J., Lin K.L., “Removal of Cu²⁺ from wastewater using eco-hydroxyapatite synthesized from marble sludge”, *Materials Chemistry and Physics*, 293, (2023), 126854.
- [15]. Wei W., Li J., Han X., Yao Y., Zhao W., Han R., Li S., Zhang Y., Zheng C., “Insights into the adsorption mechanism of tannic acid by a green synthesized nano-hydroxyapatite and its effect on aqueous Cu(II) removal”, *Science of Total Environment*, 778, (2021), 146189.
- [16]. Leeson L.J., Krueger J.E., Nash R.A., “Concerning the structural assignment of the second and third acidity constants of tetracycline antibiotics”, *Letters Tetrahedron*, 4, (1963), 1155–1160.
- [17]. Chen Y., Wang F., Duan L., Yang H., Gao J., “Tetracycline adsorption onto rice husk ash, an agricultural waste: Its kinetic and thermodynamic studies”, *Journal of Molecular Liquids*, 222, (2016), 487–494.
- [18]. Laabd M., Brahmi Y., El Ibrahim B., Hsini A., Toufik E., Abdellaoui Y., Abou Oualid H., El Ouardi M., Albourine A., “A novel mesoporous hydroxyapatite@montmorillonite hybrid composite for high-performance removal of emerging ciprofloxacin antibiotic from water: Integrated experimental and Monte Carlo computational assessment”, *Journal of Molecular Liquids*, 338, (2021), 116705.
- [19]. Chang P.H., Li Z., Jean J.S., Jiang W.T., Wang C.J., Lin K.H., “Adsorption of tetracycline on 2:1 layered non-swelling clay mineral illite”, *Applied Clay Science*, 67-68, (2012), 158-163.
- [20]. Chang P.H., Jean J.S., Jiang W.T., Li Z., “Mechanism of tetracycline sorption on rectorite”, *Colloids and Surfaces A*, 339, (2009), 94-99.
- [21]. Li Z., Schulz L., Ackley C., Fenske N., “Adsorption of tetracycline on kaolinite with pH-dependent surface charges”, *Journal of Colloid and Interface Science*, 351, (2010), 254-260.
- [22]. Borthakur P., Aryafard M., Zara Z., David R., Minofar B., Das M.R., Vithanage M., “Computational and experimental assessment of pH and specific ions on the solute solvent interactions of clay-biochar composites towards tetracycline adsorption: Implications on wastewater treatment”, *Journal of Environmental Management*, 283, (2021), 111989.
- [23]. Afzal M.Z., Yue R., Sun X.F., Song C. Wang S.G., “Enhanced removal of ciprofloxacin using humic acid modified hydrogel beads”, *Journal of Colloid and Interface Science*, 543, (2019), 76–83.
- [24]. Parker H.L., Hunt A.J., Budarin V.L., Shuttleworth P.S., Miller K.L., Clark J.H., “The importance of being porous: polysaccharide-derived mesoporous materials for use in dye adsorption,” *RSC Advances*, 2, (2012), 8992.
- [25]. Laabd M., El Jaouhari A., Bazzaoui M., Albourine A., El Jazouli H., “Adsorption of benzene-polycarboxylic acids on the electrosynthesized polyaniline films: ^[1]_[SEP]Experimental and DFT calculation,” *Journal of Polymers and Environment*, 25, (2017), 359–369.
- [26]. Peng X., Hu F., Dai H., Xiong Q., Xu C., “Study of the adsorption mechanisms of ciprofloxacin antibiotics onto graphitic ordered mesoporous carbons”, *Journal of Taiwan Institute of Chemical Engineers*, 65, (2016), 472–481. ^[1]_[SEP]
- [27]. Abdellaoui Y., Abou Oualid H., Hsini A., El Ibrahim B., Laabd M., El Ouardi M., Giacomán-Vallejos G.,

Gamero-Melo P., “Synthesis of zirconium- modified Merlinoite from fly ash for enhanced removal of phosphate in aqueous medium: Experimental studies

supported by Monte Carlo/SA simulations”, *Chemical Engineering Journal*, 404, (2021), 126600.